

The effect of an external torque on low to high confinement transitions

D. E. Newman and B. A. Carreras
Oak Ridge National Laboratory, Oak Ridge, Tennessee 37831-8070

P. H. Diamond
University of California at San Diego, La Jolla, California 92093-0319

(Received 14 October 1994; accepted 1 May 1995)

A number of experiments have attempted, with varying degrees of success, to influence the low to high confinement mode (L–H) transition through the application of an external flow shear forcing mechanism. In order to theoretically describe this type of experiment, an external torque is included in the phase transition model of Diamond *et al.* [Phys. Rev. Lett. **72**, 2965 (1994)] for the L–H bifurcation. These equations exhibit a bifurcation between an L-mode fixed point and an H-mode fixed point with variation of a critical parameter, corresponding to the edge gradient, across a threshold value. With the addition of the external torque [from biased limiter, probe, or radio frequency (rf) wave], the character of the transition changes in a manner analogous to the addition of an external magnetic field to a ferromagnetic material. In addition to the change in the transition dynamics, there is a marked decrease in the threshold level. In this simple model, the decrease in threshold level is proportional to the applied torque to the two-thirds power, in approximate functional agreement with that seen by some experiments. © 1995 American Institute of Physics.

I. INTRODUCTION

The L–H transition has now been observed in a wide range of toroidal magnetic confinement devices with a variety of triggering mechanisms [i.e., neutral beam heating, Ohmic heating, and radio frequency (rf) heating]. A universal feature of this transition seems to be the formation of a layer of radial electric field shear and a concomitant reduction in fluctuations and transport. The causal relationship between the different elements has been difficult to verify experimentally because of the speed with which the transition usually occurs. Nevertheless, much progress has been made both experimentally and theoretically in understanding the dynamics. A simple self-consistent model, coupling the poloidal shear flow with the fluctuations through a combination of Reynolds stress as a source of the shear flow and shear suppression of the turbulent fluctuations, was developed in Ref. 1. In this phase transition model, the radial inhomogeneity of the fluctuations combines with an anisotropy, due to any seed flow, to drive shear flow through the Reynolds stress. This shear flow then suppresses the fluctuations, causing a barrier to fluctuation-driven transport and further steepening the local gradients. In order to investigate the mechanism for the formation of the shear layer, some experiments^{2–5} have used limiter or probe biasing to form a local gradient in the radial electric field. These experiments are difficult to interpret in detail, but do show that the transition threshold from a low confinement (L) mode to a high confinement (H) mode is affected by the modest external torques imposed by the biasing. In addition to the modification of the threshold, the experiments show an asymmetry in the effect of the torque. This asymmetry usually manifests itself as a preferred direction in which a smaller applied torque causes a larger change in threshold.

In order to investigate the effect of torque on the phase transition model, an external torque term is added to the poloidal momentum balance equation. It is found, analyti-

cally and computationally, that an applied torque can modify both the transition dynamics and threshold level. This study is limited to modest applied torques to maintain the self-consistency of the model. The form of the torque is kept general in order to investigate the dynamical effects independent of torque models.⁶ In order to include large induced fields, one must include the evolution of the pressure gradient (∇P) in the transition model. In this extended model (including the ∇P evolution), which will be presented in detail in a later publication,⁷ the asymmetry of the change in power threshold due to an applied torque can also be seen.⁸ The effect of the torque suggests that it could be used to move the system between the L and H regimes and, in this way, possibly control the transport barrier.

The remainder of this paper is organized as follows. In Sec. II, the model and some of its applications are briefly reviewed. In Sec. III we discuss the changes in the transition due to the external torque, followed by the variation of the threshold due to the torque in Sec. IV. In Sec. V, the conclusions are presented, including a brief mention of some results from the further extension (including ∇P evolution) of the model (given in detail elsewhere).

II. BASIC MODEL

The model derived in Ref. 1 describes the evolution of the fluctuation energy and the poloidal velocity shear. As presented in Ref. 1, the model is radially local and assumes modest sheared E_r in order to allow the $E \times B$ shear flow to be approximated by the poloidal shear flow. This restriction is removed in the extension to the model mentioned earlier. Here the basic model is extended to include an external torque driving the shear flow,

$$\frac{1}{2} \frac{dE}{dt} = \gamma_0 E - \alpha_1 E^2 - \alpha_2 U^2 E, \quad (1)$$

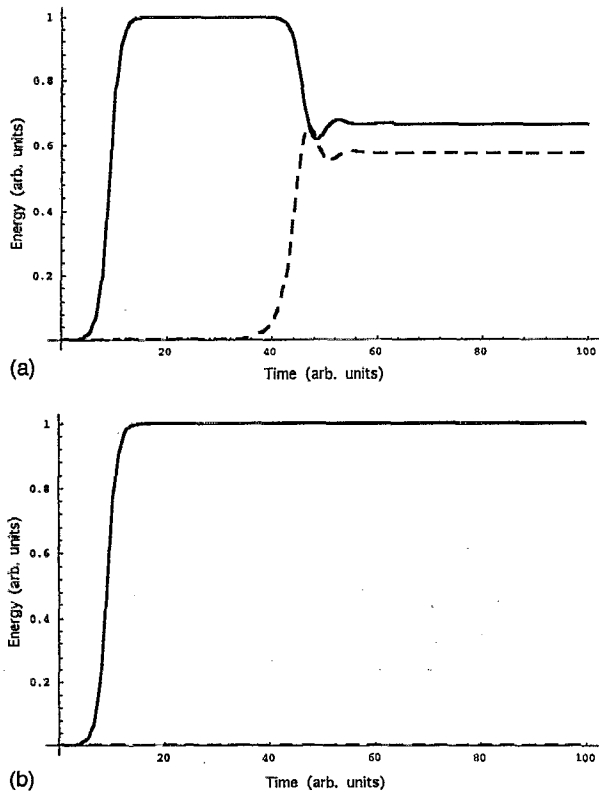


FIG. 1. (a) Shows the evolution of the fluctuation energy (solid line) and the shear flow (dashed line) as a function of time for a supercritical set of parameters ($a/b=1.5$). Note that the system first evolves to an "L" mode followed by a transition to the "H"-mode state. (b) Shows the evolution for the same two quantities with a subcritical parameter set ($a/b=0.5$). Note there is no transition to the "H"-mode state.

$$\frac{dU}{dt} = -\mu U + \alpha_3 U E + \tau_{\text{ext}}, \quad (2)$$

with $E = |\tilde{n}_k/n_0|^2$ the fluctuation energy, $U = \langle V_E' \rangle$ the flow shear, and τ_{ext} the external torque. The coefficients γ_0 , α_1 , α_2 , μ , and α_3 are dependent on the specific fluctuation model and are examined in Refs. 1 and 2. In the absence of the external torque, the dynamics of the system depended on only two parameters: $a = \alpha_3/\alpha_1$ and $b = \mu/\gamma_0$, with $a/b=1$ being the threshold for the transition. For values of a/b less than 1, all of the free energy goes into the fluctuations, and no shear flow is generated. By increasing the parameter above the threshold value, the instability saturates first at the L-mode level and then there is a smooth transition to the H mode with generation of flow (Fig. 1). With the addition of the external forcing term (τ_{ext}), the two states remain relatively unchanged with the addition of a small L-mode torque-driven shear flow. This small, externally driven flow has little effect on the fluctuation levels until the external torque approaches within an order of magnitude of a/b . There are, however, two important effects that follow from even a small amount of external torque. These are changes in the character of the transition dynamics and in the threshold value for the transition. In the regime very close to the transition point, the system dynamics are dominated by the shear

flow. In this case, the two fields can be reduced to one by slaving the fluctuation energy to the flow, resulting in an equation for the flow given by

$$\frac{dU}{dt} = \left(\frac{\alpha_3 \gamma_0}{\alpha_1} - \mu \right) U + \frac{\alpha_3 \alpha_2}{\alpha_1} U^3 + \tau_{\text{ext}}.$$

This equation is equivalent to the Landau model for second-order phase transitions and has many of the same characteristics.

III. CHARACTER OF TRANSITION CHANGES WITH TORQUE

We define the critical point and susceptibility for the L-H transition in a manner similar to that encountered in the theory of transitions in the presence of an external field (followed by Landau and Lifshitz⁹). In the external torque-free case, this is relatively simple because the first derivative of each field (U and E) is discontinuous. However, with the addition of the torque this discontinuity is removed. A definition that works in both limits is needed, and is provided by the maximum of the susceptibility function. The linear susceptibility is $\chi = |dU/d\tau|_{a,b}$; therefore, the critical point (a_{crit}) is defined as the point at which $d\chi/da=0$ (with χ positive). Here χ is singular in the torque-free limit, but the changes smoothly when an external torque is added. Using this definition of the critical point, one can investigate the dynamics of the critical point as a function of torque both analytically and computationally.

In order to simplify the notation we nondimensionalize the equations, which results in

$$\frac{1}{2} \frac{d\hat{E}}{dt} = \hat{E} - \hat{E}^2 - \hat{U}^2 \hat{E}, \quad (3)$$

$$\frac{d\hat{U}}{dt} = -b \hat{U} + a \hat{U} \hat{E} + \tau, \quad (4)$$

with a and b as defined earlier and $\hat{E} = \sqrt{\alpha_1/\gamma_0} E$, $\hat{U} = \sqrt{\alpha_2/\gamma_0} U$, and $\tau = \sqrt{\alpha_2/\gamma_0^3} \tau_{\text{ext}}$. Then the equations for the fixed points become

$$\hat{E} - \hat{E}^2 - \hat{U}^2 \hat{E} = 0, \quad (5)$$

$$-b \hat{U} + a \hat{U} \hat{E} + \tau = 0. \quad (6)$$

For this set of equations there is a zero fluctuation level solution given by $\hat{E}=0$ and $\hat{U}=\tau/b$. The other solutions satisfy

$$a \hat{U}^3 - (a-b) \hat{U} - \tau = 0. \quad (7)$$

For \hat{E} to remain positive, the solutions for \hat{U} must have $\hat{U}^2 < 1$, which implies that if \hat{U} becomes > 1 , there exists a transition to the trivial solution that cannot exist in the torque-free case. For τ vanishing, the solutions become the same as those given in Ref. 1 for the L and H modes. Unlike the torque-free case, in which the derivative of the roots is discontinuous across the transition, the roots for Eq. (7) continuously connect the "old" L- and H-mode solutions. For $a=b$, the solution to Eq. (7) is $\hat{U} = (\tau/a)^{1/3}$. For $a < b$ (the L-mode region), the approximate solution is $\hat{U} \approx \tau/(a-b)$,

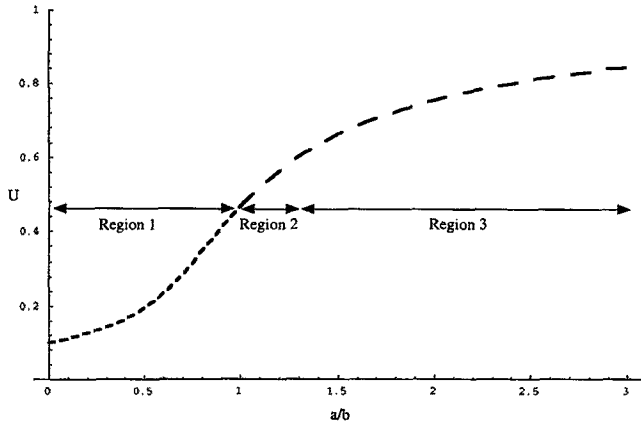


FIG. 2. Flow shear versus a/b from the three solutions to Eq. (7). The three regions are delineated by arrows and dashed or solid lines. The fine dashed line is the solution in region 1, the solid dashed line in region 2, and the coarse dashed line in region 3.

whereas for $a > b$ there are two regions. These regions are $\tau/a > 2/3\sqrt{3}\tau(1-b/a)^{3/2}$ and $\tau/a \leq 2/3\sqrt{3}\tau(1-b/a)^{3/2}$. In the first of these regions, the solution is

$$\hat{U} = \frac{2}{\sqrt{3}}\sqrt{1-b/a} \cosh\left[\frac{1}{3} \operatorname{arccosh}\left(\frac{3\sqrt{3}\tau}{2a(1-b/a)^{3/2}}\right)\right].$$

This region disappears when τ vanishes. The second region has the solution

$$\hat{U} = \frac{2}{\sqrt{3}}\sqrt{1-b/a} \sin\left[\frac{\pi}{3} + \frac{1}{3}\operatorname{arcsin}\left(\frac{3\sqrt{3}\tau}{2a(1-b/a)^{3/2}}\right)\right].$$

and goes to $\sqrt{1-b/a}$ (the torque-free H-mode solution) as τ goes to 0. These analytic solutions to Eq. (7) are shown in Fig. 2, and the regions are delineated by the arrows.

Using the definition of χ given in the beginning of the section on Eq. (7) gives

$$\chi = \frac{\hat{U}}{(3\hat{U}^2 a - a + b)},$$

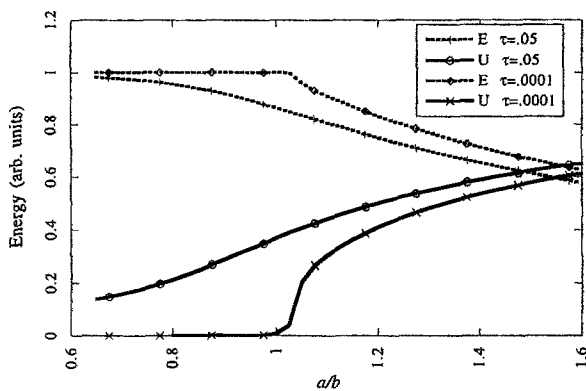


FIG. 3. We see \hat{E} and \hat{U} as functions of a/b for two values of external torque. Note the sharp transition for the small torque case and the smoothed transition for the larger torque case.

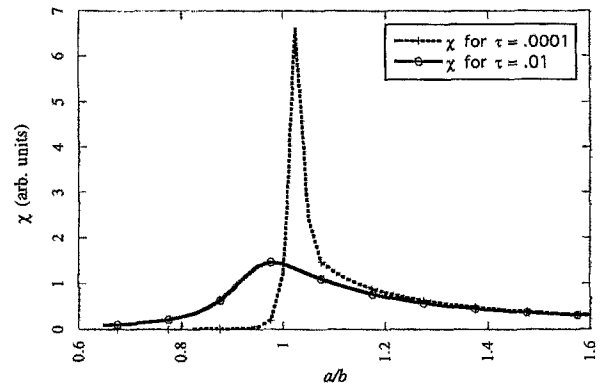


FIG. 4. Here χ vs a is plotted, showing the changing character of the transition for larger torques.

which is no longer singular at the critical point due to the nonzero \hat{U} on the L-mode side of the transition. Figure 3 shows the change in \hat{E} and \hat{U} as a function of the parameter a for two different values of external torque. For very small τ , the transition is sharp (almost discontinuous) and becomes explicitly discontinuous in the zero torque limit. The larger the torque, the smoother and more spread out the transition becomes. The susceptibility (χ) is shown in Fig. 4, and the smoothing of the transition can be seen more clearly. However, it can also be seen that there is a well-defined maximum in χ . It is this maximum that we will now investigate.

VI. VARIATION OF THRESHOLD WITH TORQUE FOR SIMPLE MODEL

It is apparent from Fig. 4 that the external torque not only broadens the transition but also shifts the maximum to a lower value of a . The dependence of the threshold on the external torque can be seen more clearly in the derivative of the susceptibility with respect to the parameter a (Fig. 5). Here the threshold is the zero crossing and can be seen to move from near 1 for the small value of applied torque to nearly 0.96 for the larger τ . This is the same type of behavior that is seen in experiments² when an external torque is applied.

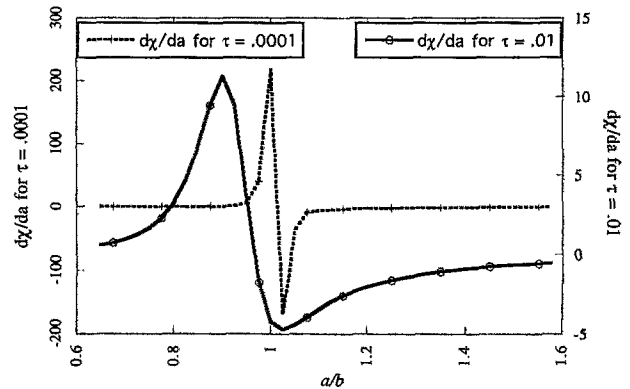


FIG. 5. Here $d\chi/da$ vs a/b for large and small values of external torque. Note the shift of the zero crossing (the critical point) for the larger value of the torque.

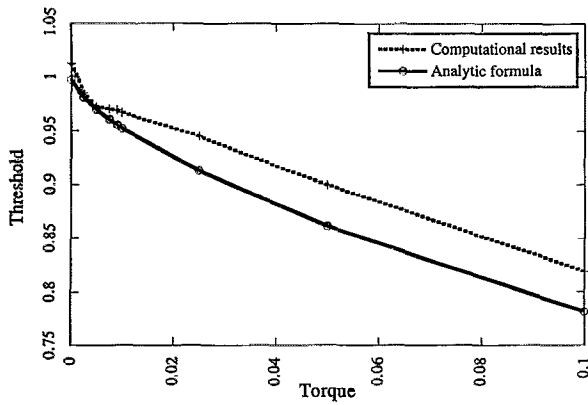


FIG. 6. Critical point versus applied torque.

If we solve for U in the equation $d\chi/da=0$, with χ coming from Eq. (8), we find $\hat{U}=(b-a/3a)^{1/2}$. Substituting this into Eq. (7) gives a relation between a , b , and τ at the threshold:

$$b_{\text{crit}} = a + a^{1/3} \left(\frac{\sqrt{3} \cdot 3}{4} \tau \right)^{2/3} \quad (9)$$

or

$$\gamma_{0\text{crit}} = \frac{\mu\alpha_1}{\alpha_3} - \left(\frac{27}{16} \frac{\alpha_2\alpha_1^2}{\alpha_3^2} \tau_{\text{ext}}^2 \right)^{1/3}. \quad (10)$$

It can be seen from Eq. (10) that the threshold is reduced by $\tau^{2/3}$, with the application of an external torque. This, in turn, leads to a reduction of the power threshold (with the same functional form). This relationship is apparent in Fig. 6, which plots the threshold, as determined for $d\chi/da=0$ versus the applied torque. An applied dimensionless torque on the order of 10% of the critical parameter can give a change in the threshold as large as 20%. Also plotted in Fig. 6 is the analytical expression for the threshold as a function of the torque. Although the curves do not correspond exactly, they do appear to be functionally similar. Finally, it should be noted that when the external torque is large enough so that τ/b is larger than 1, the stable solution is the zero fluctuation level solution: $\hat{E}=0$ and $\hat{U}=\tau/b$. This is simply a statement that if the external forcing is large enough, the fluctuations can be suppressed without any Reynolds stress drive. However, this requires a very large torque. The power required to produce such a torque is of comparable magnitude to the torque-free critical power.

V. CONCLUSION

The two-field phase transition model has been extended to allow an external torque. The results from this extension show a significant effect on the dynamics and a reduction of the transition thresholds due to the applied torque. The transition is seen to change from a discontinuous transition to a smooth one in the same manner as standard second-order phase transition models in the presence of an external field. The threshold is found to decrease with applied torque in

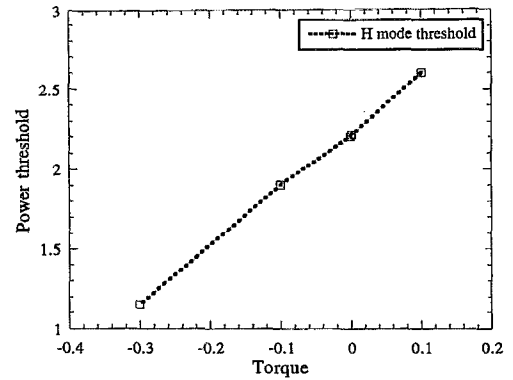


FIG. 7. Critical power versus applied torque in the extended (three-field) case. Note that the critical power is not symmetric around zero torque due to a direction favored by the pressure gradient in the three-field model.

qualitative agreement with some experimental results. The change in threshold is proportional to the applied torque to the two-thirds power.

In order to allow for a more faithful representation of the dynamics and include a wider range of parameters, the basic model has been further extended by including the evolution of ∇P . Although this extension is discussed in detail elsewhere, a bifurcation with many of the same characteristics, but of a different transition type from that observed in the two-field phase transition model, is seen in the extended (three-field) system. In addition to the already observed dynamics, the extended model allows an additional type of transition that is controlled by the relative magnitudes of the pressure-gradient-driven flow and the Reynolds-stress-driven $E \times B$ shear flow. Due to the symmetry-breaking effect of the ∇P evolution, the system is no longer symmetric in its response to an applied torque (Fig. 7). However, the functional response of the system to the external torque is similar to that reported in the two-field system. This asymmetric response to external applied torques is similar to that seen experimentally as shown in Figs. 1 and 3 of Ref. 2.

ACKNOWLEDGMENTS

Valuable discussions with J. N. Leboeuf are gratefully acknowledged. D. E. Newman would like to thank Oak Ridge National Laboratory for its support through the Wigner Fellowship program.

This work was sponsored by the Office of Fusion Energy, U.S. Department of Energy under Contract No. DE-AC05-84OR21400 with Martin Marietta Energy Systems, Inc.

¹P. H. Diamond, Y-M. Liang, B. A. Carreras, and P. W. Terry, *Phys. Rev. Lett.* **72**, 2565 (1994).

²R. R. Weynants, D. L. Hillis, J. A. Boedo, G. Tynan, R. Van Nieuwenhove, G. Van Oost, G. Bertschinger, R. W. Conn, K. H. Dippel, F. Durodié, H. Euringer, K. H. Finken, D. S. Gray, J. T. Hogan, L. Könen, A. M. Messiaen, P. K. Mioduszewski, J. Ongena, A. Pospieszczyk, U. Samm, B. Schweer, R. Sporcken, G. Telesca, P. E. Vandenplas, and G. H. Wolf, in *Proceedings of the 14th International Conference on Plasma Physics and Controlled Nuclear Fusion Research* (International Atomic Energy Agency, Vienna, 1992), Vol. 1, p. 251.

³R. R. Weynants and G. Van Oost, *Plasma Phys. Controlled Fusion B* **35**, 177 (1993).

- ⁴S. Ohdachi, T. Shoji, K. Nagashima, H. Tamai, Y. Minsa, H. Maeda, H. Toyama, and the JFT-2M Group, *Plasma Phys. Controlled Fusion A* **36**, 201 (1994).
- ⁵L. Schmitz, H. Kugel, R. Bell, R. Doerner, G. Tynan, L. Blush, M. Okabayashi, R. Kaiti, R. W. Conn, and the PBX-M Group, *Proceedings of International Atomic Energy Agency Workshop on Tokamak Biasing Experiments*, Montreal, September 1992 (International Atomic Energy Agency, Vienna, 1993), p. 285.
- ⁶K. Itoh, *Plasma Phys. Controlled Fusion A* **36**, 307 (1994).
- ⁷B. A. Carreras, D. E. Newman, P. H. Diamond, and Y.-M. Liang, *Phys. Plasmas* **1**, 4014 (1994).
- ⁸B. A. Carreras, P. H. Diamond, Y.-M. Liang, V. Lebedev, and D. Newman, *Plasma Phys. Controlled Fusion A* **36**, 93 (1994).
- ⁹L. D. Landau and E. M. Lifshitz, *Statistical Physics*, 3rd ed. (Pergamon, New York, 1986), Part 1.